

## Structure and chemical bond of carbodiylide complexes [W(CO)<sub>5</sub>{C(ECp\*)<sub>2</sub>}] (E = B to Tl): DFT calculations

Nguyen Thi Ai Nhung

Department of Chemistry, Hue University of Sciences, Hue University, Hue, Vietnam

Received 2 March 2017; Accepted for publication 20 October 2017

### Abstract

The bonding of the carbodiylide complexes [(CO)<sub>5</sub>W-{C(ECp\*)<sub>2</sub>}] (**W5-C1E**) was calculated at the BP86 level with the basis sets def2-SVP, def2-TZVPP, and TZ2P+. The nature of the (CO)<sub>5</sub>W-{C(ECp\*)<sub>2</sub>} bonds was analyzed by energy decomposition method. The calculated structures of complexes show that all ligands C(ECp\*)<sub>2</sub> (**C1E**) are bonded in a tilted orientation relative to the fragment W(CO)<sub>5</sub> in **W5-C1E** and the tilting angle become much more acute when E becomes heavier. Analysis of the bonding reveals that [(CO)<sub>5</sub>W-{C(E'Cp\*)<sub>2</sub>}] donation in **W5-C1B** come from the  $\sigma$ -lone-pair orbital of C(BCp\*)<sub>2</sub>, while [(CO)<sub>5</sub>W-{C(E'Cp\*)<sub>2</sub>}] donation in the strongly tilted bonded complexes when E' = Al to Tl comes from the  $\pi$ -lone-pair orbital of the carbodiylides C(E'Cp\*)<sub>2</sub>. The W-C bonds have not only (CO)<sub>5</sub>W←C(ECp\*)<sub>2</sub> strong  $\sigma$ -donation but also a significant contribution  $\pi$ -donation and the trend of the W-C bond strength in **W5-C1E** complexes. EDA-NOCV calculations reveal that C(ECp\*)<sub>2</sub> ligands in **W5-C1E** complexes are strong  $\sigma$ -donors and weak  $\pi$ -donors which make them good spectator ligands that are well-suited for synthesizing robust catalysts for a variety of applications.

**Keywords.** Carbodiylides, energy decomposition analysis, bond dissociations energy, bonding analysis.

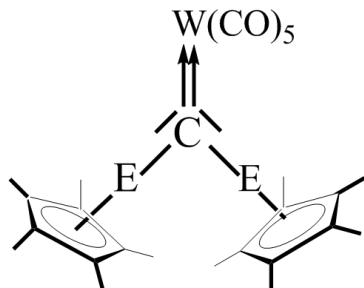
### 1. INTRODUCTION

The recent experimental studies of main-group elements pentamethylcyclopentadienyl (Cp\*) suggested that the steric requirements of the  $\sigma$ - or  $\pi$ -bound Cp\* group enable the kinetic stabilization of highly reactive species and represents a very important substituent [1]. Moreover, the chemistry of Cp\* with transition metal complexes has advanced significantly in the fields of organometallic catalysis [2-4]. The chemistry of group-13 diyl ligand ECp\* (E = B to Tl) is a topic of interest to both synthetic and theoretical chemists [5-8]. Transition metal (TM) complexes with ECp\* ligands have been the subject of extensive experimental and theoretical investigations of the first stable complex [(CO)<sub>4</sub>Fe-{AlCp\*}] which was isolated and characterized by X-ray analysis in 1997 by Fischer et al. [5]. Further work was reported with group-13 homologues [(CO)<sub>4</sub>Fe-{ECp\*}], where E = B and Ga [6, 7]. Very recently, the first homoleptic complex with an ECp\* substituent [Mo(GaCp\*)<sub>6</sub>], was synthesized [9]. Numerous other group-13 complexes with ligands ER, where R is either a strong  $\pi$  donor or a very bulky substituent, have since been reported [1, 5]. Theoretical studies clearly showed that diyl ligands ER were strong  $\sigma$

donor and weaker  $\pi$ -acceptors than CO [10]. It has been known that there is another class of stable carbones CL<sub>2</sub>, where L is a group-13 diyl ligand ECp\* (E = B to Tl), that has been studied in the recent past [10, 11]. Theoretical studies clearly showed that the diyl ligand ECp\* is a stronger  $\sigma$ -donor and weaker  $\pi$ -acceptor than CO [11, 12], and ECp\* was considered as a ligand for stabilizing a divalent carbon(0) atom in carbodiylides C(ECp\*)<sub>2</sub>. The coordination chemistry of monovalent group-13 elements has received significant attention and is presently a topic of intensive experimental research [7-13]. The diyl ligand ER where the coordinated atom E has the formal oxidation state +1 is analogous to CO [11-14]. Numerous other group-13 complexes with ER such as model ligands ECp, EN(SiH<sub>3</sub>)<sub>2</sub>, and ECH<sub>3</sub> [10, 11] where R is either a strong  $\pi$  donor or a very bulky substituent, and their electronic structures have been analyzed.

This paper provides the detailed calculations on quantum-chemical investigations of the model complexes [(CO)<sub>5</sub>W-{C(ECp\*)<sub>2</sub>}] (**W5-C1E**) where E = B to Tl (Scheme 1). The aim of the study presented in this study was to investigate the nature of bonding and extent of  $\sigma$  and  $\pi$  interactions between ligands C(ECp\*)<sub>2</sub> and the TM fragment

$W(CO)_5$  (scheme 1). The structures of the complexes and the bond dissociation energies are predicted with DFT. The electronic structures determined by charge- and energy decomposition analysis of the systems are also presented.



Scheme 1: Complexes investigated in this study:  $[(CO)_5W-C(CEp^*)_2]$  **W5-C1E** (E = B to Tl)

## 2. COMPUTATIONAL METHODS

Geometry optimizations of the molecules have been carried out without symmetry constraints using the Gaussian03 [15] optimizer together with Turbomole 6.0.1 [16] energies and gradients at the BP86 [17, 18] /def2-SVP [19] level of theory (denoted BP86/SVP). For the heavier group-13 atoms In, Tl, and for W, small-core quasi-relativistic effective core potentials (ECPs) were used [20]. The stationary points on the potential energy surface (PES) obtained at this level of theory was denoted as BP86/def2-SVP. All structures presented in this study turned out to be minima on the PES. Single point calculations with the same functional but the larger def2-TZVPP [21] basis set and the small core ECPs for In, Tl and W atoms were carried out with Gaussian03 on the structures derived on BP86/def2-SVP level of theory. The bond dissociation energies and molecular orbitals were calculated and plotted at the BP86/TZVPP//BP86/SVP level of theory using the NBO 3.1 program [22, 23]. The complexes were re-optimized for the EDA-NOCV with the program package ADF 2009.01 [24] with BP86 in conjunction with a triple-z-quality basis set using uncontracted Slater-type orbitals (STOs) augmented by two sets of polarization function, with a frozen-core approximation for the core electrons [25]. An auxiliary set of *s*, *p*, *d*, *f*, and *g* STOs was used to fit the molecular densities and to represent the Coulomb and exchange potentials accurately in each SCF cycle [26]. Scalar relativistic effects were incorporated by applying the zeroth-order regular approximation (ZORA) [27]. The calculations have been carried out at the BP86/TZ2P+ level of theory on the BP86/def2-SVP optimized geometries which were used for the bonding analysis in term of the

EDA [28]-NOCV [29] method of  $C_1$  symmetric geometries.

## 3. RESULTS AND DISCUSSION

The optimized geometries of **W5-C1B** to **W5-C1TI** complexes and free **C1B** to **C1TI** ligands are shown in Figure 1. The theoretically predicted W-C bond length decreases from **W5-C1B** (2.434 Å) to **W5-C1TI** (1.989 Å). The equilibrium geometries of **W5-C1B** to **W5-C1TI** in Figure 1 shows that only the ligand **C1B** has the B1 atom  $\eta_1$ -bonded to the central C atom which the longest and shortest B1-C bonds of Cp\* ring are 3.420 and 1.577 Å, while the B2 atom is  $\eta_3$ -bonded to the central C atom with longest and shortest bond of 2.308 and 1.649 Å, respectively. In contrast, the Al atoms in **W5-C1Al** are both  $\eta_5$ -bonded to the central C atom of the respective Cp\* rings, which have values between 2.222 and 2.237 Å, while the heavier homologues  $C(CEp^*)_2$  where E = Ga to Tl, suggest that there is a trend toward bonding between  $\eta_3$  and  $\eta_1$  for E-Cp\* when E becomes heavier. This remains the five E-C bonds to the carbon atoms of the Cp\* ligand which exhibit between 2.272 and 2.364 Å for **W5-C1Ga**, 2.495 and 2.802 Å for **W5-C1In**, and 2.748 and 2.845 Å for **W5-C1TI**. The bending angle,  $\alpha$ , is 156.9° in **W5-C1B** and becomes much more acute in the heavier homologues which the value decreases from  $\alpha = 138.3^\circ$  in **W5-C1Al** to  $\alpha = 132.8^\circ$  in **W5-C1Ga** and then increases a bit for **W5-C1In** 135.8°, and is 138.7° for **W5-C1TI**. This means all ligands are bonded in a tilted orientation to  $W(CO)_5$  in the complexes. This implies that there is not only a possible interaction with the  $\sigma$ -lone-pair of **C1E**, but also with the  $\pi$ -lone-pair [10, 11, 32]. Figure 1 also shows the optimized geometries of free  $C(CEp^*)_2$  molecules. There is a significant difference between boron compound **C1B** and the heavier homologues. The former has a nearly linear B1-C-B2 moiety (178.5°), whereas the latter, the heavier species, are strongly bent. The bending angle, E-C-E, of the heavier homologues varies between 101.1° for **C1Ga** and 104.5° for **C1TI**. The calculated bending angles are clearly smaller than those in  $C(NHC_{Me})_2$  (131.8°) and in  $C(PPh_3)_2$  (136.9°) [30]. The geometry of  $C(BCp^*)_2$  suggests that the compound can be considered as a substituted homologue of  $HB=C=BH$ , which has been synthesized by laser-ablated of boron atoms with methane in a low-temperature matrix by Andrews [31]. The boron atoms are  $\eta_1$ -bonded to one carbon atom of the Cp\* ligand. The calculated B1-C and B2-C bonds in  $C(BCp^*)_2$  are 1.380 Å. The interatomic B-C

distances to the other carbon atoms of the ring are much longer [32], and should not be considered as genuine boron-carbon bonds. The C-C bonds in the Cp\* groups, which are rotated with respect to each other by about 90° around the C-B-C axis, show the characteristic pattern of alternating distances in a 1,3-butadiene moiety that are bonded to the carbon atoms of Cp\* rings, which exhibit between 1.553 and 3.177 Å [32]. This situation is strikingly different to the C-C bonds in the Cp\* rings of C(AlCp\*)<sub>2</sub>, which have nearly identical values between 1.442 and 1.445 Å. The same trend holds for each of the five Al-C bonds to the carbon atoms of the Cp\* ligand, which lie between 2.259 and 2.273 Å. The calculated equilibrium structure of C(AlCp\*)<sub>2</sub> clearly shows that the Cp\* ligands are η<sub>5</sub>-bonded to aluminum with calculated Al1-C and Al2-C bonds of 1.844 and 1.843 Å. The optimized geometries of the remaining homologues C(ECp\*)<sub>2</sub>, where E = Ga, In, and Tl, suggests that there is a trend toward η<sub>3</sub> or η<sub>1</sub> bonding for E-C (Cp\* rings) when E becomes heavier. This becomes obvious by an increasing distortion of the cyclic ligands toward bond alternation of the C-C distances in the ring and particularly by the differences among the E-C bonds

to the Cp\* ligand. The ligand in C(GaCp\*)<sub>2</sub> have one short (2.066 Å) Ga1-C bond, two rather long Ga-C bonds (2.449 and 2.472 Å), and two very long Ga-C distances (3.002 and 3.023 Å). The GaCp\* bonding can be interpreted as intermediate between η<sub>3</sub> and η<sub>1</sub>. Note that the similar situation is found for the indium and thallium ligands C(InCp\*)<sub>2</sub> and C(TlCp\*)<sub>2</sub>. A comparison between the geometry of **W5-C1B** to **W5-C1TI** and the free ligands **C1B** to **C1TI** shows that the E-C bonds in all ligands **CE** are clearly longer in complexes **W5-C1B** to **W5-C1TI** (0.4 to 0.7 Å) than those in the free ligands. Note that free C(BCp\*)<sub>2</sub> ligand has a nearly linear B1-C-B2 moiety (178.5°), whereas the ligand in the complex has a bent B1-C-B2 moiety (150.1°). The calculated B1-C and B2-C bonds in **C1B** are 1.380 Å, which is slightly longer than the calculated values of 1.374 Å for the linear equilibrium structure of HB=C=BH at BP86/SVP [33]. The calculated B1-C and B2-C bonds in **W5-C1B** are 1.403 and 1.424 Å. The optimized geometries of the free ligands in figure 1, together with the calculated values for the most important bond lengths and angles, are similar to the calculated values of carbodiylides C(ECp\*)<sub>2</sub> investigated recently [32].

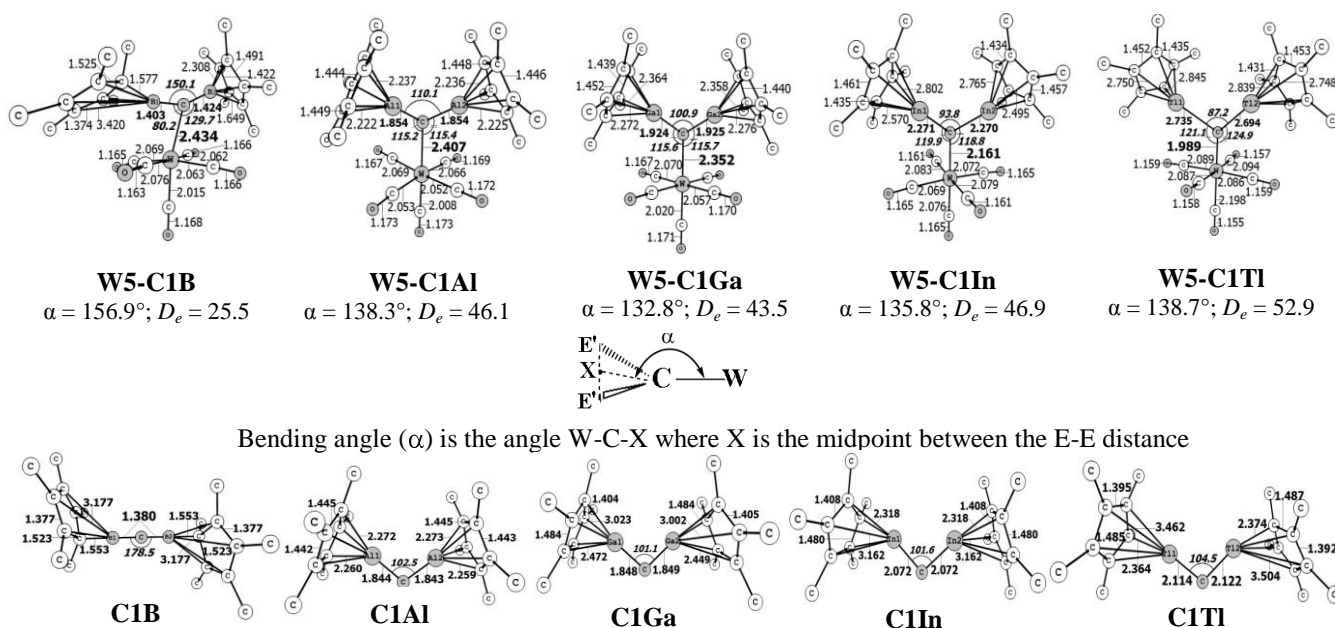


**Figure 1:** Optimized geometries of the complexes **W5-C1E** and the free ligands **C1E** at the BP86/def2-SVP level. Bond lengths are given in Å; angles in degrees. Calculated metal-ligand BDEs,  $D_e$  (kcal/mol), at the BP86/def2-TZVPP/BP86/def2-SVP level for the (CO)<sub>5</sub>W-C(ECp\*)<sub>2</sub> bonds (E = B to Tl)

Figure 1 also gives the theoretically predicted bond dissociation energies (BDEs) for the W-C bond of **W5-C1B** to **W5-C1TI** and exhibit an interesting non-steric trend. The calculated bond energies suggest that the tungsten-carbodiylides bond strength increases from **W5-C1B** to **W5-C1Al**, decreases for

E = Ga, and then increases again for **W5-C1In** and **W5-C1TI**. The data thus suggest that the heavier complexes have stronger bonds than the lighter homologues. Continuously, the EDA-NOCV calculations give a more insight into the nature of metal-ligand bonding in **W5-C1B** to **W5-C1TI**.

Table 1 shows the numerical results of EDA-NOCV calculations for the  $(\text{CO})_5\text{W}$ -carbodiylide bonds. The EDA-NOCV data demonstrates that the increase in metal-ligand bonding comes from the intrinsic interactions  $\Delta E_{\text{int}}$ , which clearly increases from **W5-C1B** to **W5-C1TI**. The intrinsic interaction in **W5-C1Ga** is even smaller than that in **W5-C1Al** and increases for the heavier homologues. The increase of  $\Delta E_{\text{int}}$  from **W5-C1B** to **W5-C1Al** is not as steep as the BDE, which strongly increases from **W5-C1B** to **W5-C1Al**. This is because the aluminum complex has a significantly smaller preparation energy of  $\Delta E_{\text{prep}}=8.7$  kcal/mol, while for the boron complex it

is  $\Delta E_{\text{prep}} = 23.1$  kcal/mol. From this, it follows that linear  $\text{Cp}^*\text{B}=\text{C}=\text{BCp}^*$  has to be bent in complex **W5-C1B**. The small decrease of the BDEs ( $D_e$ ) from **W5-C1Al** (45.0 kcal/mol) to **W5-C1Ga** (42.8 kcal/mol) is due to the small increase in the preparation energy  $\Delta E_{\text{prep}}$  and the small decrease in  $\Delta E_{\text{int}}$  for the complexes. In contrast, the increase of  $D_e$  in **W5-C1E** (E = Ga to Tl) comes from the larger intrinsic interactions  $\Delta E_{\text{int}}$  (-52.2 kcal/mol for **W5-C1Ga** to -66.5 kcal/mol for **W5-C1TI**), and are nearly canceled out by the preparation energies  $\Delta E_{\text{int}}$  in the complexes.

Table 1: EDA-NOCV results at the BP86/TZ2P+ level for complexes **W5-C1B** to **W5-C1TI** using the moieties  $[\text{W}(\text{CO})_5]$  and  $[\text{C}(\text{ECp}^*)_2]$  as interacting fragments. The complexes were analyzed with  $C_1$  symmetry. Energy values in kcal/mol

Compound	<b>W5-C1B</b>	<b>W5-C1Al</b>	<b>W5-C1Ga</b>	<b>W5-C1In</b>	<b>W5-C1TI</b>
Fragments	$\text{W}(\text{CO})_5$ $\text{C}(\text{BCp}^*)_2$	$\text{W}(\text{CO})_5$ $\text{C}(\text{AlCp}^*)_2$	$\text{W}(\text{CO})_5$ $\text{C}(\text{GaCp}^*)_2$	$\text{W}(\text{CO})_5$ $\text{C}(\text{InCp}^*)_2$	$\text{W}(\text{CO})_5$ $\text{C}(\text{TlCp}^*)_2$
$\Delta E_{\text{int}}$	-48.7	-53.7	-52.2	-64.6	-66.5
$\Delta E_{\text{Pauli}}$	100.3	101.6	102.4	148.0	156.1
$\Delta E_{\text{elstat}}^{[a]}$	-92.4 (62.0 %)	-95.2 (61.3 %)	-92.3 (59.7 %)	-128.5 (57.7 %)	-133.6 (62.8 %)
$\Delta E_{\text{orb}}^{[a]}$	-56.6 (38.0 %)	-60.1 (38.7 %)	-62.3 (40.3 %)	-79.0 (42.4 %)	-94.1 (37.2 %)
$\Delta E_{\sigma}^{[b]}$	-35.9 (63.4 %)	-42.3 (70.3 %)	-45.0 (72.2 %)	-61.1 (78.0 %)	-76.7 (81.5 %)
$\Delta E_{\pi}^{[b]}$	-18.0 (31.8 %)	-15.0 (24.9 %)	-13.8 (22.2 %)	-14.5 (18.3 %)	-14.3 (15.2 %)
$\Delta E_{\text{rest}}^{[b]}$	-2.7 (4.8 %)	-2.8 (4.8 %)	-3.5 (5.6 %)	-2.9 (3.7 %)	-3.1 (3.3 %)
$\Delta E_{\text{prep}}$	23.1	8.7	9.4	17.5	18.2
$\Delta E(= -D_e)$	-25.6 (-25.5) <sup>[c]</sup>	-45.0 (-46.1) <sup>[c]</sup>	-42.8 (-43.5) <sup>[c]</sup>	-47.1 (-46.9) <sup>[c]</sup>	-48.3 (-52.4) <sup>[c]</sup>

<sup>[a]</sup>The values in parentheses are the percentage contributions to the total attractive interactions  $\Delta E_{\text{elstat}} + \Delta E_{\text{orb}}$ ; <sup>[b]</sup>The values in parentheses are the percentage contributions to the total orbital interactions  $\Delta E_{\text{orb}}$ ; <sup>[c]</sup>The values in parentheses give the dissociation energy at the BP86/def2-TZVPP//BP86/def2-SVP level.

The three main terms  $\Delta E_{\text{Pauli}}$ ,  $\Delta E_{\text{elstat}}$ , and  $\Delta E_{\text{orb}}$  are considered to inspect their contribution to the interaction energy  $\Delta E_{\text{int}}$  of the molecules. Inspection of the three main terms indicated that the Pauli repulsion  $\Delta E_{\text{Pauli}}$  was similar for the lighter species where E = B, Al, and Ga and became larger for the heavier atoms when E = In and Tl. This can be explained that the increase in the bond strength for the heavier carbodiylides comes from the stronger attraction rather than weaker repulsion [33]. The attractive interactions  $\Delta E_{\text{elstat}}$  increase from **W5-C1B** to **W5-C1TI** except for the small decrease from **W5-C1Al** to **W5-C1Ga**. The increase in the attractive interactions  $\Delta E_{\text{elstat}}$  and  $\Delta E_{\text{orb}}$  of the heavier carbodiylide ligands can be traced back to the  $\sigma$ -lone-pair orbital, which leads to stronger  $\sigma$ -orbital interactions  $\Delta E_{\sigma}$  and to stronger electrostatic attraction  $\Delta E_{\text{elstat}}$ . Inspection of the trend of the electrostatic term  $\Delta E_{\text{elstat}}$ , and the orbital term  $\Delta E_{\text{orb}}$  shows that the stronger bonds are mainly caused by

the latter term. The  $\sigma$ -orbital contribution  $\Delta E_{\sigma}$  is much stronger for the heavier carbodiylides which means they increase from **W5-C1B** to **W5-C1TI**. In contrast, the  $\pi$ -orbital contributions  $\Delta E_{\pi}$  are much weaker than those of  $\Delta E_{\sigma}$  and decrease for the heavier group-13 diyl ligands. The  $\Delta E_{\text{orb}}$  term of the EDA-NOCV results was examined further to obtain more detailed information on the bonding in **W5-C1B** to **W5-C1TI**. Figures 2 shows plots of those pairs of orbitals  $\psi_k/\psi_{-k}$  that yield the NOCVs with the largest contributions to the  $\sigma$ - and  $\pi$ -orbital terms  $\Delta E_{\sigma}$  and  $\Delta E_{\pi}$  in **W5-C1B** and **W5-C1TI**. The associated deformation densities,  $\Delta\rho$ , and stabilization energies are also given. The adducts **W5-C1Al**, **W5-C1Ga**, and **W5-C1TI** exhibit similar shapes to those of the complex **W5-C1TI**. Therefore, the NOCV pairs of **W5-C1Al**, **W5-C1Ga** and **W5-C1In** are not shown in Figures 2. Note that the green/red colors for  $\psi_k/\psi_{-k}$  indicate the sign of the orbitals, while the yellow/blue colors in the

deformation densities,  $\Delta\rho$  indicate the charge flow. The yellow areas of  $\Delta\rho$  designate present charge depletion while the blue areas indicate charge accumulation. The charge flow  $\Delta\rho$  takes places in the direction yellow→blue. Figure 2a gives the NOCV pairs  $\psi_1/\psi_{-1}$  and the deformation densities  $\Delta\rho_1$  of the most important pair of  $s$  orbitals for  $\Delta E_\sigma$  of **W5-C1B**. The associated stabilization energies of  $\Delta\rho_1$  are approximately 90% of the total energies  $\Delta E_\sigma$  (Table 2). Thus, the orbital pairs  $\psi_1/\psi_{-1}$  can be considered as dominant sources of  $s$  bonding for the **C1B** ligands in the two complexes. The shape of the orbital pairs clearly indicates that  $\sigma$ -orbital interactions take place between the donor orbitals of **C1B** ligands, and the acceptor orbital of  $W(CO)_5$ . Note that the charge flow  $(CO)_5W \leftarrow C(ECp^*)_2$  involves not only donor C and acceptor W atoms. In particular, there is charge flow into the W-CO bonding and C-O anti-bonding regions, particularly for the trans-CO bond, which agrees with the change in the bond lengths between  $W(CO)_6$  and **W5-C1E**. Figure 2-a clearly shows that the  $\sigma$ -type interaction has clearly the direction  $(CO)_5W \leftarrow C(ECp^*)_2$ . The deformation density reveals that the charge flow comes from the  $C(ECp^*)_2$  ligands ( $E = B$ ) toward the  $W(CO)_5$  fragment; this is in good agreement with the calculated partial charges which were shown in Table 1. The NOCV pairs were analyzed for the  $W(CO)_5$ -carbodiylides because the ligands  $C(ECp^*)_2$  are double donors, and there should be no significant contribution from  $(CO)_5W \rightarrow C(ECp^*)_2$   $\pi$ -back-donation. Figure 2-b and 2-c show that two NOCV pairs  $\psi_k/\psi_{-k}$  ( $k = 2, 3$ ) dominate the total stabilization  $\Delta E_\pi$  in **W5-C1B**. The shape of the NOCV pairs  $\psi_2/\psi_{-2}$  and the deformation densities, which reveal the charge flow  $\Delta\rho_2$ , are shown in Figure 2-b and indicate that the stabilization of -8.7 kcal/mol can be assigned to the  $(CO)_5W \rightarrow C(BCp^*)_2$   $\pi$ -backdonation where the C-B vacant anti-bonding orbital serves as acceptor. This contributes to the weakening of the C-B bonds, which become longer in **W5-C1B** than that of the free ligand. In contrast, figure 2-c shows the shape of the charge flow  $\Delta\rho_3$ , which indicates that the stabilization of -3.7 kcal/mol comes mainly from relaxation of the  $W(CO)_5$  fragment. The EDA-NOCV results for **W5-C1TI**, which are shown from Figures 2-d to 2-f, are interesting because they give detailed insight into the bonding situation of the tilted bonded thallium complex, which exhibits the shortest W-C bond of the lighter species. Figures 2-d, and 2-e show that the  $\sigma$ -type interaction have surprising pairs in either the direction of  $(CO)_5W \leftarrow C(TICp^*)_2$   $\sigma$ -donation or

$(CO)_5W \rightarrow C(TICp^*)_2$  backdonation in the **W5-C1TI** complex. The shapes of the  $\psi_{-1}$  and  $\psi_{-2}$  donor fragment of the NOCV pairs of **W5-C1TI** suggest that the  $\sigma$ -donation comes from the **C1TI** ligand toward the  $W(CO)_5$  fragment. The acceptor fragment  $\psi_1$  of **W5-C1TI** looks very similar to the  $\sigma$ - acceptor fragment of **W5-C1B** (Figure 2-a) together with the shapes of the  $\psi_{-1}$  donor fragment. However, the shape of the  $\psi_2/\psi_{-2}$  acceptor fragment of the NOCV pair of **W5-C1TI** suggests that  $\sigma$ -donation comes from the HOMO of  $C(TICp^*)_2$ , which has  $\pi$ -symmetry with respect to the free ligand. The deformation densities  $\Delta\rho_1$  and  $\Delta\rho_2$ , which indicate stabilization of -49.5 and -21.2 kcal/mol, and not only exhibit a significant area of charge donation (yellow area) from the **C1TI** fragment toward the  $W(CO)_5$  moiety, but also exhibit an area of charge backdonation (blue area) from  $(CO)_5W$  to  $C(TICp^*)_2$ . Figure 2-f shows very weak  $\pi$ -type orbital interactions in **W5-C1TI**, which indicate that the stabilization of  $\Delta\rho_3 = -11.4$  kcal/mol comes mainly from typical  $\pi$ -back-donation  $(CO)_5W \rightarrow C(TICp^*)_2$ . The bonding analysis in continuously examined by considering the molecular orbitals with the energy levels of the energetically highest lying  $\sigma$  and  $\pi$  orbitals of **C1E** ligands.

Figure 3 shows the shape of the energetically highest-lying occupied orbitals HOMO and HOMO-1. These MOs of  $C(BCp^*)_2$  exhibit the shape of a nearly degenerate pair of orbitals that have approximate  $\pi$ -symmetry. HOMO and HOMO-1 are strongly delocalized over the whole molecule, and thus, do not resemble lone-pair orbitals. In contrast to this, the highest-lying occupied MOs of  $C(AlCp^*)_2$  are easily identified as  $\pi$ -lone pair (HOMO) and  $\sigma$ -lone-pair (HOMO-1) orbitals at the carbon atom. This weakly attractive E-C-E interaction leads to the rather acute bonding angle. A similar situation of  $C(AlCp^*)_2$  is found for the HOMO and HOMO-1 of the heavier homologues  $C(ECp^*)_2$  ( $E = Ga$  to  $Tl$ ). The main difference is that the HOMO-1 in the heavier species has increased contributions from the  $\pi$ -orbitals of the  $Cp^*$  moieties. Figure 3 also shows the energy levels of the two highest-lying occupied MOs which have  $\sigma$ - or  $\pi$ -symmetry of the ligands  $C(ECp^*)_2$ . The energies of the  $\pi$ -orbitals get lower in energy from Al to Ga, and then they increase slightly from Ga to Tl. The  $\sigma$ -orbitals are lower in energy than the  $\pi$ -orbitals and become lower in energy when E changes from Al to Ga, and then nearly do not change in energy. The lower energy of the  $\sigma$ -lone-pairs is one reason for the change to tilted bonding

of the  $C(ECp^*)_2$  ligands. We realize that  $\sigma$ -donation  $[(CO)_5W \leftarrow \{C(ECp^*)_2\}]$  in the latter complexes takes place from the  $\pi$ -lone-pair orbitals of the ligands  $C(ECp^*)_2$ , which have pure  $\pi$ -character. There is some  $s/p$  hybridization at the carbon donor atom in the complexes that becomes smaller when the bending angle,  $\alpha$ , becomes more acute. The carbodiylides  $C(ECp^*)_2$  have two lone-pair orbitals,

but they can use their  $\pi$ -lone-pair electrons for donor-acceptor interactions in the side-on complexes. The increase in the donation  $(CO)_5W \leftarrow C(ECp^*)_2$ , which is manifested in the calculated values for  $\Delta E_\sigma$  and electrostatic attraction  $\Delta E_{elstat}$  provides a rationale for the stronger bonding of the ligands  $C(ECp^*)_2$  when E becomes heavier.

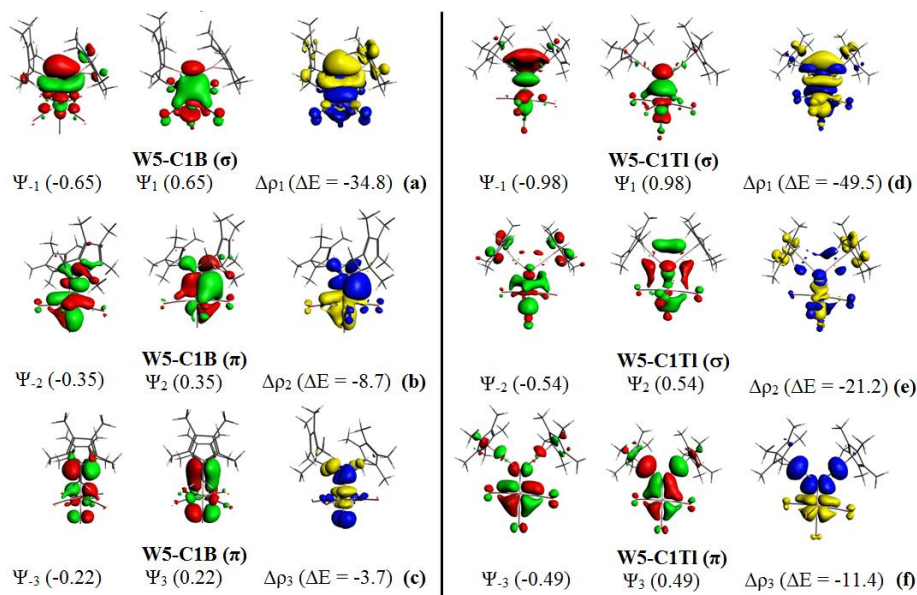


Figure 2: Most important NOCV pairs of orbitals  $\psi_{-k}$ ,  $\psi_k$  with their eigenvalues  $-v_k$ ,  $v_k$ , which is given in parentheses, and the associated deformation densities,  $\rho_k$ , and orbital stabilization energies,  $\Delta E$ , for the complex **W5-C1B** and **W5-C1TI**. The charge flow in the deformation densities is from the yellow  $\rightarrow$  blue region. (a)  $\sigma$ -NOCV of **W5-C1B**; (b) and (c)  $\pi$ -NOCVs of **W5-C1B**. (d) and (e)  $\sigma$ -NOCVs of **W5-C1TI**; (f)  $\pi$ -NOCV of **W5-C1TI**. Energy values in kcal/mol

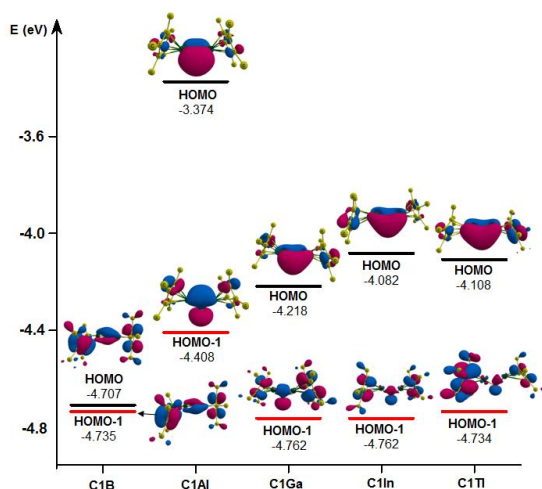


Figure 3: Plot of the energy levels of the energetically highest lying  $\sigma$  and  $\pi$  orbitals of free ligands **C1E**

#### 4. CONCLUSION

The calculated structures of the **W5-C1E** complexes show that ligands **C1E** are bonded in an arrangement that is tilted with respect to the metal fragment  $W(CO)_5$ . The theoretical calculation of BDEs suggests that the bond strength of complexes increases from the boron complex **W5-C1B** to the strongest bonded thallium adduct **W5-C1TI**. Analysis of the bonding situation reveals that the  $(CO)_5W \leftarrow C(BCp^*)_2$  donation in **W5-C1B** comes from the  $\sigma$ -lone-pair orbital of  $C(BCp^*)_2$ , while the donation  $(CO)_5W \leftarrow C(ECp^*)_2$  in the strongly tilted bonding complexes where  $E = Al$  to  $Tl$  comes from the  $\pi$ -lone-pair orbital of the carbodiylides  $C(ECp^*)_2$ . The EDA-NOCV results suggest that the trend of the W-C bond strength **W5-C1B** < **W5-C1Al** < **W5-C1Ga** < **W5-C1In** < **W5-C1TI** comes from the increase in  $(CO)_5W \leftarrow C(ECp^*)_2$  donation

and from lower preparation energies than that of **W5-C1B** and the carbodiylides ligands  $C(ECp^*)_2$  in the complexes **W5-C1E** are strong  $\sigma$ -donors and weak  $\pi$ -donors.

**Acknowledgements.** *Nguyen Thi Ai Nhung especially thanks Prof. Dr. Gernot Frenking and Dr. Ralf Tonner for their support and helpful discussion. The program of the studies was run via the Erwin cluster operated by Reuti at the Philipps-Universität Marburg-Germany.*

## REFERENCES

1. D. Weiss et al. *[(dcpe)Pt(ECp\*)<sub>2</sub>] (E = Al, Ga): Synthesis, Structure, and Bonding Situation of the First Aluminum(I) and Gallium(I) Complexes of Phosphine-Substituted Transition Metal Centers*, *Organometallics*, **19**(22), 4583-4588 (2000).
2. Y. Bunno, N. Murakami, Y. Suzuki, M. Kanai, T. Yoshino, S. Matsunaga, *Cp\*Co<sup>III</sup>-Catalyzed Dehydrative C–H Allylation of 6-Arylpurines and Aromatic Amides Using Allyl Alcohols in Fluorinated Alcohols*, *Org. Lett.*, **18** (9), 2216-2219 (2016).
3. K. Fujimura, M. Ouchi, J. Tsujita, M. Sawamoto. *Cationic Cp\*-Ruthenium Catalysts for Metal-Catalyzed Living Radical Polymerization: Cocatalyst-Independent Catalysis Tuned by Counteranion*, *Macromolecules*, **49**(8), 2962-2970 (2016).
4. S. Figueiredo et al. *Bis(pyrazolyl)methanetetracarbonyl-molybdenum(0) as precursor to a molybdenum(VI) catalyst for olefin epoxidation*, *J. Organomet. Chem.* **723**, 56-64 (2013).
5. J. Weiss, D. Stetzkamp, B. Nuber, R. A. Fischer, C. Boehme, G. Frenking, *[( $\eta^5$ -C<sub>5</sub>Me<sub>5</sub>)Al-Fe(CO)<sub>4</sub>] Synthesis, Structure, and Bonding*, *Angew. Chem. Int. Ed. Engl.*, **36**(12), 70-72 (1997).
6. J. Su, X.-W. Li, R. C. Crittendon, C. F. Campana, G. H. Robinson, *Experimental Confirmation of an Iron–Gallium Multiple Bond: Synthesis, Structure, and Bonding of a Ferrogallyne*, *Organometallics*, **16**(21), 4511-4513 (1997).
7. A. H. Cowley, V. Lomeli, A. Voigt, *Synthesis and Characterization of a Terminal Borylene (Borandiyl) Complex*, *J. Am. Chem. Soc.*, **120**(25), 6401-6402 (1998).
8. T. A. N. Nguyen et al. *Structures and Bonding Situation of Iron Complexes of Group-13 Half-Sandwich ECp\* (E = B to Tl) Based on DFT Calculations*, *Z. Anorg. Allg. Chem.*, **642**(8), 609-617 (2016).
9. T. Cadenbach, T. Bollermann, C. Gemel, I. Fernandez, M. von Hopffgarten, G. Frenking, R. Fischer. *Twelve One-Electron Ligands Coordinating One Metal Center: Structure and Bonding of [Mo(ZnCH<sub>3</sub>)<sub>9</sub>(ZnCp\*)<sub>3</sub>]*, *Angew. Chem. Int. Ed.*, **47**(47), 9150-9154 (2008).
10. C. Boehme, J. Uddin, G. Frenking. *Chemical bonding in mononuclear transition metal complexes with Group 13 diyl ligands ER (E=B-Tl): Part X: Theoretical studies of inorganic compounds*, *Coord. Chem. Rev.*, **197**(1), 249-276 (2000).
11. J. Uddin, G. Frenking. *Energy Analysis of Metal-Ligand Bonding in Transition Metal Complexes with Terminal Group-13 Diyl Ligands (CO)<sub>4</sub>Fe-ER, Fe(EMe)<sub>5</sub> and Ni(EMe)<sub>4</sub>(E = B–Tl; R = Cp, N(SiH<sub>3</sub>)<sub>2</sub>, Ph, Me) Reveals Significant  $\pi$  Bonding in Homoleptical Molecules*, *J. Am. Chem. Soc.*, **123**(8), 1683-1693 (2001).
12. J. Uddin, C. Boehme, G. Frenking. *Nature of the Chemical Bond between a Transition Metal and a Group-13 Element: Structure and Bonding of Transition Metal Complexes with Terminal Group-13 Diyl Ligands ER (E = B to Tl; R = Cp, N(SiH<sub>3</sub>)<sub>2</sub>, Ph, Me)*, *Organometallics.*, **19**(4), 571-582 (2000).
13. J. Weiss, D. Stetzkamp, B. Nuber, R. A. Fischer, C. Boehme, G. Frenking. *[( $\eta^5$ -C<sub>5</sub>Me<sub>5</sub>)Al-Fe(CO)<sub>4</sub>]-Synthesis, Structure, and Bonding*, *Angew. Chem. Int. Ed. Engl.*, **36**(12), 70-72 (1997).
14. R. Kinjo, B. Donnadiou, M. A. Celik, G. Frenking, G. Bertrand. *Synthesis and Characterization of a Neutral Tricoordinate Organoboron Isoelectronic with Amines*, *Science*, **333**(6042), 610-613 (2011).
15. Gaussian 03, Revision D.01. M. J. Frisch, J. A. Pople, Gaussian Inc., Wallingford, CT, **2004**.
16. R. Ahlrichs, M. Bär, M. Häser, H. Horn, C. Kölmel. *Electronic structure calculations on workstation computers: The program system turbomole*, *Chem. Phys. Lett.*, **162**(3), 165-169 (1989).
17. A. D. Becke. *Density-functional exchange-energy approximation with correct asymptotic behavior*, *Phys. Rev. A*, **38**(6), 3098-3100 (1988).
18. J. P. Perdew. *Density-functional approximation for the correlation energy of the inhomogeneous electron gas*, *Phys. Rev. B*, **33**(12), 8822-8824 (1986).
19. A. Schäfer, H. Horn, R. Ahlrichs. *Fully optimized contracted Gaussian basis sets for atoms Li to Kr*, *J. Chem. Phys.*, **97**(4), 2571 (1992).
20. F. Weigend, R. Ahlrichs. *Balanced basis sets of split valence, triple zeta valence and quadruple zeta valence quality for H to Rn: Design and assessment of accuracy*, *Phys. Chem. Chem. Phys.*, **7**(18), 3297 (2005).
21. B. Metz, H. Stoll, M. Dolg. *Small-core multiconfiguration-Dirac–Hartree–Fock-adjusted pseudopotentials for post-d main group elements: Application to PbH and PbO*, *J. Chem. Phys.*, **113**(7), 2563 (2000).
22. A. E. Reed, L. A. Curtiss, F. Weinhold. *Intermolecular interactions from a natural bond orbital, donor-acceptor viewpoint*, *Chem. Rev.*, **88**(6), 899-926 (1988).
23. K. Wiberg. *Application of the pople-santry-segal CNDO method to the cyclopropylcarbiny and cyclobutyl cation and to bicyclobutane*, *Tetrahedron*, **24**(3), 1083-1096 (1968).
24. G. te Velde et al. *Chemistry with ADF*, *J. Comput. Chem.*, **22**(9), 931-967 (2001).

25. J. G. Snijders, E. J. Baerends, P. Vernooijs. *Roothaan-Hartree-Fock-Slater atomic wave functions: Single-zeta, double-zeta, and extended Slater-type basis sets for<sub>87</sub>Fr-<sub>103</sub>Lr*, At. Data. Nucl. Data Tables, **26(6)**, 483-509 (1982).
26. J. Krijn, E. J. Baerends. *Fit Functions in the HFS-Method, Internal Report*, Vrije Universiteit Amsterdam, The Netherlands (1984).
27. E. van Lenthe, A. Ehlers, E. J. Baerends. *Geometry optimizations in the zero order regular approximation for relativistic effects*, J. Chem. Phys., **110(18)**, 8943 (1999).
28. T. Ziegler, A. Rauk. *CO, CS, N<sub>2</sub>, PF<sub>3</sub> and CNCH<sub>3</sub> as  $\sigma$  donors and  $\pi$  acceptors. A theoretical study by the Hartree-Fock-Slater transition-state method*, Inorg. Chem., **18(7)**, 1755-1759 (1979).
29. A. Michalak, M. Mitoraj, T. Ziegler. *A Combined Charge and Energy Decomposition Scheme for Bond Analysis*, J. Chem. Theory. Comput., **5(4)**, 962-975 (2009).
30. R. Tonner, G. Frenking. *Divalent Carbon(0) Chemistry, Part I: Parent Compounds*, Chem. Eur. J., **14(11)**, 3260-3272 (2008).
31. P. Hassanzadeh, L. Andrews. *Reactions of pulsed laser evaporated boron atoms with methane. 1. Synthesis and characterization of a novel molecule with carbon-boron double bonds: HBCBH*, J. Am. Chem. Soc., **114(23)**, 9239-9240 (1992).
32. S. Klein and G. Frenking. *Carbodiylides C(ECp\*)<sub>2</sub> (E = B - Tl): Another Class of Theoretically Predicted Divalent Carbon(0) Compounds*, Angew. Chem. Int. Ed., **49(39)**, 7106-7110 (2010).
33. W. A. Herrmann, M. Denk, J. Behm, W. Scherer, F.-R. Klingan, H. Bock, B. Solouki, M. Wagner. *Stable Cyclic Germanediyls ("Cyclogermynes"): Synthesis, Structure, Metal Complexes, and Thermolyses*, Angew. Chem. Int. Ed. Engl., **31(11)**, 1485-1488 (1992).

Corresponding author: **Nguyen Thi Ai Nhung**

Hue University of Sciences, Hue University  
No. 77, Nguyen Hue, Hue City, Thua Thien Hue Province  
E-mail: nguyenainhung.hueuni@gmail.com.